⌘ *Author's Choice*

THE JOURNAL OF BIOLOGICAL CHEMISTRY VOL. 284, NO. 32, pp. 21307–21316, August 7, 2009

High Yield Heterologous Expression of Wild-type and Mutant Cu^+-ATPase (ATP7B, Wilson Disease Protein) for Functional Characterization of Catalytic Activity and Serine Residues Undergoing Copper-dependent Phosphorylation*

Received for publication, May 20, 2009, and in revised form, June 8, 2009 Published, JBC Papers in Press, June 11, 2009, DOI 10.1074/jbc.M109.023341

Rajendra Pilankatta[‡], David Lewis[‡], Christopher M. Adams[§], and Giuseppe Inesi[‡1]

From the [‡]California Pacific Medical Center Research Institute, San Francisco, California 94107 and the [§]Stanford University Mass Spectrometry Laboratory, Stanford, California 94305

ATP7B is a P-type ATPase required for copper homeostasis and related to Wilson disease of humans. In addition to various domains corresponding to other P-type ATPases, ATP7B includes an N terminus extension (NMBD) with six copper binding sites. We obtained high yield expression of WT and mutant ATP7B in COS1 cells infected with adenovirus vector. ATP7B, isolated with the microsomal fraction of cell homogenates, accounts for 10–20% of the total protein. Copper-dependent, steady-state ATPase yields 30 nmol of P_i/mg of protein/min at 37 °C, pH 6.0. ATP7B phosphorylation with ATP occurs with diphasic kinetics and is totally copper-dependent. Alkali labile phosphoenzyme (catalytic intermediate of P-ATPases) accounts for a small fraction of the total phosphoprotein and is prevented by D1027N (P domain) or C983A/C985A (*CXC* copper binding motif in TM6) mutations. Decay of [^{32}P]phosphoenzyme following chase with non-radioactive ATP occurs with an initial burst involving alkali labile phosphoenzyme (absent in D1027N and C983A/C985A mutants) and continues at a slow rate involving alkali-resistant phosphoenzyme. If a copper chelator is added with the ATP chase, the initial burst is smaller, and further cleavage is totally inhibited. Analysis by proteolysis and mass spectrometry demonstrates that the alkali stable phosphoenzyme involves Ser^{478} and Ser^{481} (NMBD), Ser^{1121} ("N" domain) and Ser^{1453} (C terminus), and occurs with the same pattern *ex vivo* (COS-1) and *in vitro* (microsomes). The overall copper dependence of phosphorylation and hydrolytic cleavage suggests long range conformational effects, including interactions of NMBD and headpiece domains, with strong influence on catalytic turnover.

ATP7A and ATP7B are two P-type ATPases involved in copper homeostasis (1, 2), and their mutational defects in humans are responsible for Menkes or Wilson disease, respectively (3–6). In principle, the P-type denomination applies to enzymes that sustain hydrolytic cleavage of phosphorylated substrates, with a catalytic mechanism including intermediate phosphorylation of the Asp residue within an invariant DKTG motif. Although this mechanism extends to the large family of halogenases (7), "P-type ATPase" refers to membrane-bound enzymes that couple ATP utilization to cation transport, and are divided into five subfamilies depending on cation specificity and other features of structure and function (8, 9). The ATP7A and ATP7B copper ATPases are included in the P_1-subfamily, which is selective for soft and transition metals. In addition to a putative transmembrane metal binding motif (TMBS),[2] corresponding to the cation binding/transport sites of other P-ATPases, ATP7A and ATP7B possess a specific N terminus extension (NMBD) that includes six (*CXXC*) metal binding sites that may be involved in enzyme activation. Furthermore, phosphorylation of the ATP7A and ATP7B proteins may modulate the functional behavior of the enzyme, in addition to forming a catalytic intermediate (10). These specific structural features, as well as various interactions with chaperones and targeting sites, render characterization of ATP7A and ATP7B rather complex. It is useful to obtain ATP7B protein by heterologous expression in cell cultures, to perform functional characterization of the enzyme in its native form, and subsequent analysis by site-directed mutagenesis. In fact, heterologous expression in insect cells, and initial characterization, were obtained by Tsivkoskii *et al.* (11) and Hung *et al.* (12). We report here high yield expression of WT and mutant ATP7B in COS1 cells infected with adenovirus vector, and functional characterization of membrane-bound ATPase obtained with the microsomal fraction of infected cells. The microsomal protein sustains a copper-dependent steady-state ATPase rate of 30 nmol/per mg of protein per minute at pH 6 and 37 °C, in the presence of 1 mM ATP. We demonstrate by proteolysis and mass spectrometry that, in addition to the invariant DKTG motif undergoing phosphorylation as a catalytic cycle intermediate in other P-type ATPases, the recombinant enzyme undergoes copper-dependent phosphorylation of four serine residues.

* This work was supported, in whole or in part, by National Institutes of Health Grant RO301-69830 from the NHBLI.

⌘ *Author's Choice*—Final version full access.

[1] To whom correspondence should be addressed: California Pacific Medical Center Research Institute, 475 Brannan St., San Francisco, CA 94107. Tel.: 415-600-1745; Fax: 415-600-1725; E-mail: ginesi@cpmcri.com.

[2] The abbreviations used are: TMBS, transmembrane metal binding site; SERCA1, sarcoplasmic reticulum calcium ATPase; NMBD, N-terminal metal binding domain; MOPS, 3-(*N*-morpholino)propanesulfonic acid; BCS, bathocuproine disulfonate; BCA, bicinchoninic acid; MS, mass spectrometry; MS/MS, tandem MS; TM6, transmembrane 6; CMV, cytomegalovirus; PBS, phosphate-buffered saline; MES, 4-morpholineethanesulfonic acid; DTT, dithiothreitol; GFP, green fluorescent protein.

MATERIALS AND METHODS

Construction of rAdATP7Bmyc—Recombinant adenovirus vector containing CMV promoter-driven ATP7B cDNA fused with 3′ c-*myc* tag was constructed as detailed below. pCMV vector containing ATP7B cDNA purchased from Origene was digested with Not1 to release the cDNA and subcloned into pShuttleCMV vector to generate pShuttleCMV-ATP7B. pShuttleCMV-ATP7B plasmid DNA was subjected to PCR amplification at an annealing temperature of 40 °C using the following primers: forward primer, 5′-GGATATTTTGTCCCATTTAT-3′; reverse primer, 5′-ATGCAATCTAGATCACAGGTCCTCCTCTGAGATCAGCTTCTGCTCGATGTACTGCTCCTCATCCC-3′.

The PCR product was digested with Cla1/Xba1 and ligated into pShuttleCMV-ATP7B to generate pShuttleCMV-ATP7Bmyc plasmid construct (Fig. 1*A*). The reading frame of ATP7B cDNA and c-*myc* tag was confirmed by DNA sequencing. The plasmid construct, pShuttleCMV-ATP7Bmyc, was linearized with Pme1 and subjected to homologous recombination with pAdeasy-1 DNA (Ad5 genome) in BJ5183 *Escherichia coli* cells by co-electroporation (13). The resulting recombinant DNA was digested with Pac1 and transfected into HEK293 cells using Lipofectamine and PLUS reagent (Invitrogen) to package recombinant adenoviral vector construct, rAdATP7Bmyc (Fig. 1*B*). rAdATP7Bmyc was amplified in HEK 293 cells, and then single plaques were amplified again and purified by ultracentrifugation using CsCl density gradient.

Site-directed mutations, D1027N (in the DKTG motif of N-domain), C983A and C985A (in the C*X*C motif of transmembrane helix 6 (TM6), TMBS), and C575A and C578A (in the C*XX*C motif of the sixth site in the NMBD) were created in pShuttleCMV-ATP7Bmyc plasmid using a QuikChange II site-directed mutagenesis kit (Stratagene) as per the manufacturer's instructions. The mutations were confirmed by sequencing, and related plasmids were used for construction of rAdATP7Bmyc mutants.

Infection of COS-1 Cells with rAdATP7Bmyc and Immunostaining of Recombinant ATP7B—COS-1 cells were grown until 60–70% confluency in Dulbecco's modified Eagle's medium containing 10% fetal bovine serum, inside a CO_2 incubator at 37 °C in a 60-mm culture dish. The cells were infected with optimal rAdATP7Bmyc viral titers as determined by preliminary cytotoxicity and expression titrations. Following incubation for 48 or 72 h in a CO_2 incubator, the cells were detached using 0.2% trypsin-EDTA solution (Invitrogen), and re-seeded onto a sterile coverslip that was placed in a 35-mm culture dish. Following incubation at 37 °C in the CO_2 incubator for additional 5 h to obtain a uniform cell distribution, the cells were fixed with 3.7% (v/v) paraformaldehyde in PBS for 20 min, followed by permeabilization with 0.1% Triton X-100 in PBS for 15 min at room temperature. The permeabilized COS-1 cells were blocked with 10% horse serum in PBS for 1 h at room temperature followed by the incubation with diluted primary anti-*myc* monoclonal antibody (9E10) at 4 °C overnight in block solution. The primary antibodies were detected by incubating the cells with anti-mouse Alexa 488 (Invitrogen), diluted (1:200) in the block solution for 2 h at room temperature. The nuclei of the infected cells were stained with propidium iodide (10 μg/ml in PBS) for 10 min. Each step was followed by three times rinsing with PBS. Finally, the stained cells were evaluated for ATP7Bmyc expression using a confocal laser scanning microscope (Nikon, Eclipse TE2000-U).

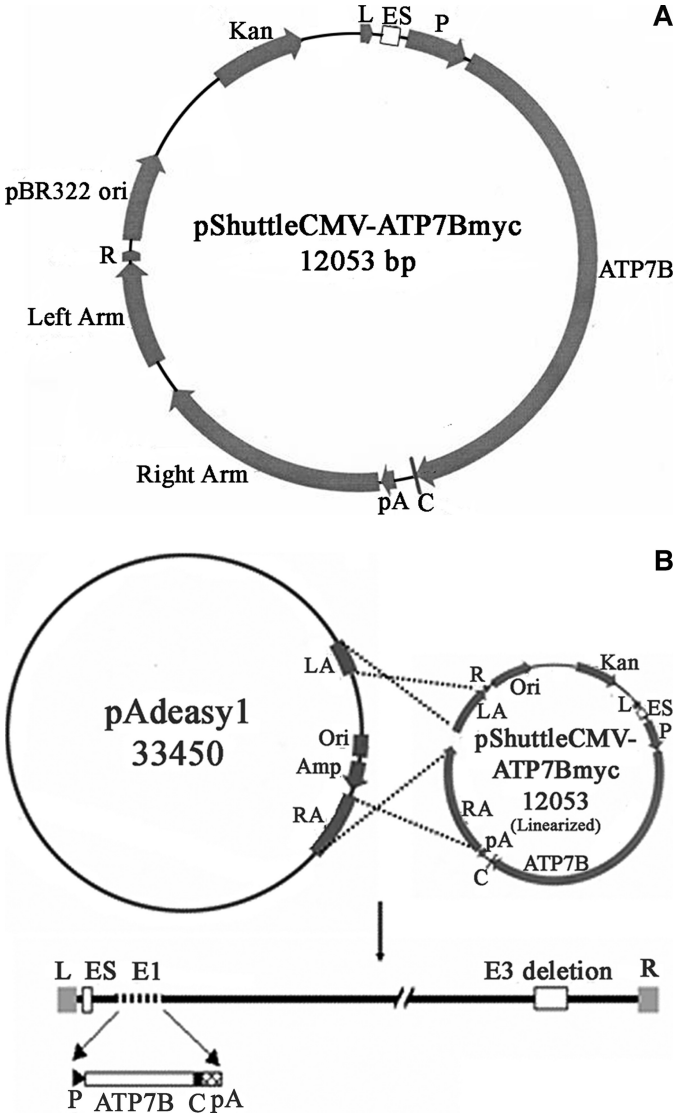

FIGURE 1. **Construction of the adenovirus vector AdATP7Bmyc: Schematic representation of the linear genome of the rAdATP7Bmyc virus.** The shuttle vector containing ATP7B cDNA, preceded by the CMV promoter and including a c-*myc* tag at the C terminus (*A*), was linearized and subjected to homologous recombination with pAdeasy1 vector (*B*). The *dashed line*, close to the *left end* represents the position of the E1, where ATP7Bmyc was inserted. The *open box* located toward the *right end* indicates a 2.7-kb deletion in the non-essential E3 region. The *shaded boxes* at either end represent the *left* (*L*) and *right* (*R*) inverted terminal repeats (*ITRs*), and the *open box* close to the *L-ITR* represents the encapsidation signal (*ES*). Components of the expression cassette are as follows: *P*, CMV promoter; *ATP7B*, ATP7B cDNA; *C*, c-*myc* tag; and *pA*, SV40 polyadenylation signal.

Microsomal Preparation—Confluent cells (infected as described above) from twenty 150-mm plates were washed twice with 10 ml of cold PBS each. The cells were then scraped off from the plates using a Teflon spatula into ice-cold PBS containing 10 mM EDTA (10 ml for 5 plates), and the scraped plates were rinsed again with PBS/EDTA (10 ml for 5 plates). The combined cell suspension was distributed in conical tubes

and centrifuged at 2,200 rpm in a clinical centrifuge for 5 min at 4 °C. The sediment was washed with PBS and centrifuged again. The sedimented cells were resuspended in 24 ml in 10 mM $NaHCO_3$ and 0.2 mM $CaCl_2$. The cells were then disrupted by explosive decompression (14), using a Parr cell disruption bomb for 5 min at 600 p.s.i. The suspension was slowly released into a collection flask containing an equal volume of 0.5 M sucrose, 0.3 M KCl, 6 mM $MgCl_2$, and 200 mM histidine, pH 7.4. Following a 20-min centrifugation at 1,000 × *g*, the sediment was discarded, and the supernatant was diluted with 12 ml of 0.25 M sucrose, 2.5 M KCl, 2 mM $MgCl_2$, 30 mM histidine, pH 7.4, and centrifuged at 10,000 × *g* for 20 min. This supernatant was centrifuged at 100,000 × *g* for 30 min. The sediment was resuspended in 30 ml of 0.25 M sucrose, 0.6 M KCl, 2 mM $MgCl_2$, 30 mM histidine, pH 7.4, and centrifuged again at 100,000 × *g* for 30 min. The final pellet (microsomal fraction) was finally resuspended in 2–3 ml of 0.25 M sucrose, 10 mM MOPS, pH 7.0. All media used for suspension of sediments contained proteolytic inhibitors (Complete Mini EDTA-free mixture from Roche Applied Science), and the resuspension was completed in a hand-held glass homogenizer. All solutions were kept at ice temperature.

Total protein determination was obtained by the Pierce BCA assay. SDS gel-electrophoresis was performed by the method of Laemmli (15) at pH 8.3, or Weber and Osborn (16) at pH 6.3. The gels were either stained for detection of protein bands, or transferred to a polyvinylidene difluoride membrane for Western blotting using 9E10 monoclonal antibodies against the c-*myc* tag. Light sarcoplasmic reticulum vesicles were obtained from rabbit skeletal muscle as described by Eletr and Inesi (17).

ATPase Activity—ATPase activity was measured at 37 °C in a reaction mixture containing 50 mM MES triethanolamine, pH 6.0, 300 mM KCl, 10 mM DTT, 3 mM $MgCl_2$, and 50 μg microsomal protein/ml, in the presence or the absence of various concentrations of $CuCl_2$ or BCS. The reaction was started by the addition of 1 mM ATP, and the activity was followed in time by colorimetric determination of P_i (18).

[^{32}P]Phosphoenzyme Formation and [^{32}P]P_i hydrolytic Cleavage by Utilization of [γ-^{32}P]ATP—ATP7B (50 μg of microsomal protein/ml) was incubated with 50 μM [γ-^{32}P]ATP at 37 °C, in a reaction mixture containing 50 mM MES triethanolamine, pH 6.0, 300 mM KCl, 10 mM DTT, and 3 mM $MgCl_2$. In addition, no copper or various concentrations of $CuCl_2$ or BCS were added, as specified in the figure legends or text. Samples were quenched at serial times with 5% trichloroacetic acid and filtered through 0.45-μm Millipore filters under vacuum suction. The filtrate was removed and processed for determination of [^{32}P]P_i, following removal of [γ-^{32}P]ATP with activated charcoal, and extraction of [^{32}P]P_i with ammonium molybdate. The filters were washed three times with 0.125 N cold perchloric acid, and once with cold water. The blotted filters were solubilized with dimethylformamide and used for determination of [γ-^{32}P]phosphoenzyme by scintillation counting. Comparative experiments were performed with microsomes derived from COS-1 cells infected with rAdATP7Bmyc and cells infected with rAdGFP ("sham").

Alternatively, the above quenched samples were pelleted by centrifugation at 5000 rpm for 5 min, resuspended in pH 8.3 or 6.3 loading buffer, and separated by Laemmli (15) or Weber-Osborn (16) gel electrophoresis. The gels were dried and exposed to a phosphor screen followed by scanning using a Typhoon scanner (Amersham Biosciences).

[^{32}P]Phosphoenzyme formation was also measured in microsomes treated with λ-protein phosphatase (New England Biolabs), as per the gel scanning method mentioned above. The phosphatase treatment was carried out in 100 μl of reaction buffer (2400 units of λ-protein phosphatase, 50 mM HEPES, 100 mM NaCl, 2 mM DTT, 0.01% Brij 35, and 1 mM $MnCl_2$, pH 7.5) containing 1 mg of microsomal protein at 30 °C for 30 min. The reaction was stopped by the addition of phosphatase inhibitor mixture (Sigma). The reaction mixture was diluted to 1 ml with microsome resuspension buffer (0.25 M sucrose, 10 mM MOPS, pH 7.0), mixed well by vortexing, and centrifuged at 14,000 rpm for 15 min. The pellet was resuspended in microsome resuspension buffer to a final volume of 200 μl. A parallel incubation was carried out in the absence of λ-protein phosphatase to serve as a negative control. [^{32}P]Phosphoenzyme formation was carried out as mentioned above in the presence of phosphatase inhibitor mixture (Sigma).

In-gel Tryptic Digestion and Phosphopeptide Analysis—Approximately 100 μg of microsomal protein derived from rAd7Bmyc-infected COS-1 cells was phosphorylated as explained above and separated in a 7.5% Weber-Osborn gel (pH 6.3) as explained above. The gel was stained with GelCode Blue Stain reagent (Pierce) as per the manufacturer's instructions. The specific ATP7B band (150 kDa) was excised from the gel, based on the comparative protein separation profile of "sham" and experimental samples. The excised band was cut into small pieces (1–2 mm square) and subjected to tryptic digestion in the presence of an MS friendly surfactant (Protease Max, Promega, Madison, WI). The extracted peptides were separated using a NanoLC system (Eksigent NanoLC-2D) and infused into an LCQ DecaXP+ MS with data-dependent acquisition (top 3 peptides, dynamic exclusion 2). MS data were extracted by Bioworks 3.0, and the human NCBI data base was searched allowing for the variable modifications, phosphorylation (STY) and oxidation (M), using Mascot. Additionally, the ATPase sequence was specifically searched using the same variable modifications in Sequest. Phosphopeptides reported by both Mascot and Sequest with a probability >95% were considered. The analysis by MS (19) was performed at the Stanford University Mass Spectrometry Facility.

RESULTS

Expression of ATP7B in COS-1 Cells Infected with Adenovirus Vector—Heterologous expression of GFP-ATP7B in hepatic WIF-B infected with adenovirus vector, for microscopic studies of polarization in culture, was recently reported by Braiterman *et al.* (20). We show here (Fig. 2, *right panel*) that a very large number (nearly all) of COS-1 cells in culture are infected by the rAdATP7Bmyc virus and express recombinant ATP7B protein as revealed by immunoreactivity of the c-*myc* tag. Enlarged views show that 1 day after infection the expressed protein is localized in proximity of the nuclei, possibly in the Golgi apparatus (Fig. 2, *left upper panel*). Three days after infection, the expressed ATP7B protein has an extensive cytosolic distribu-

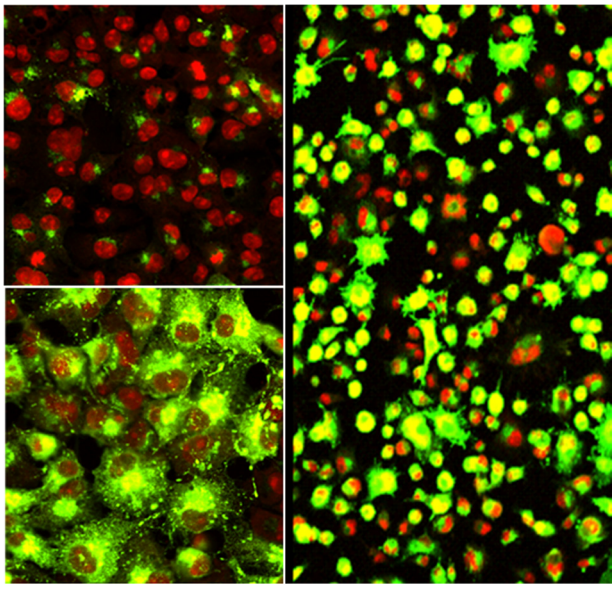

FIGURE 2. **Immunostaining of COS-1 cells infected with rAdATP7Bmyc.** *Left panel*, *upper*: cells observed 1 day after infection show expressed ATP7B protein adjacent to the nucleus, possibly in the Golgi apparatus. *Left panel*, *lower*: cells observed 3 days after infection shows expressed ATP7B protein targeted to intracellular membranes throughout the cytoplasm. *Right panel*: wide field shows that nearly all cells in culture were infected and express ATP7B, as evidenced by the *green color*. The cell nuclei of all cells are stained in *red*. Immunoreaction and staining of rAdATP7Bmyc and nuclei are as described under "Materials and Methods."

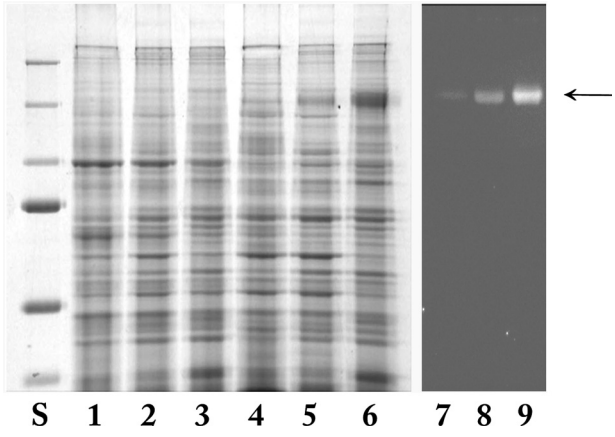

FIGURE 3. **Expression of ATP7B protein in COS-1 cells.** *Left*, electrophoretic (Laemmli) gel with stained protein where *lane S* shows molecular mass standards (250, 150, 100, 75, 50, and 37 kDa); *lanes 1–3* show fractions derived from COS-1 cells infected with adenovirus vector carrying GFP cDNA (sham); *lanes 4–6* show fractions derived from COS-1 cells infected with rAdATP7Bmyc. *Right*: the identity of the expressed ATP7B protein is demonstrated by Western blots using a monoclonal antibody specific for the c-*myc* tag. *Fractions 1*, *4*, and *7*; *2*, *5*, and *8*; and *3*, *6*, and *9* were obtained from cell homogenates, by differential centrifugation at increasing speed. *Lanes 3*, *6*, and *9* correspond to the microsomal fraction.

tion protein, evidently associated with intracellular membranes (Fig. 2, *left lower panel*). Electrophoretic analysis of three fractions obtained by differential centrifugation of homogenized cells, shows a prominent 150-kDa band associated with the microsomal fraction derived from intracellular membranes (Fig. 3, *lane 6*). This band, which accounts for 10–20% of the total protein, is specifically stained with the anti c-*myc* (tag) monoclonal antibody (Fig. 3, *lane 9*), and is hardly present in the two heavier fractions (Fig. 3, *lanes 4* and *5*). Most importantly, the band is absent in sham microsomes, obtained from cells infected with adenovirus vector carrying cDNA encoding GFP rather than ATP7B (Fig. 3, *lanes 2–4*). The catalytic and phosphorylation behavior established in the experiments described below was performed with the intracellular membrane-bound protein harvested on the third day of infection.

Steady-state ATPase Hydrolytic Activity—A rather low (1.0–1.3 μmol of P_i/mg of protein/hour) hydrolytic activity has been reported for the native Cu^+-ATPase activity associated with mouse liver microsomes (21). When we measured steady-state ATPase activity of recombinant ATP7B in various microsomal preparations of infected COS-1 cells we found values of 112 ± 49 nanomol/mg of microsomal protein/min in the presence of copper, and 81 ± 18 nmol/mg of microsomal protein/min in the presence of 1 mM BCS, at pH 6.0 and 37 °C temperature. The hydrolytic activity of sham microsomes (obtained from cells infected with adenovirus vector carrying cDNA encoding GFP rather than ATP7B) was 74 and 62 nmol/mg of microsomal protein/min in the presence of copper or BCS, respectively. Therefore, the copper-dependent steady-state activity of the microsomal protein obtained from COS-1 cells expressing ATP7B was ~30 nmol/mg/min (*i.e.* 1.8 μmol/mg/h).

ATPase Phosphorylation and P_i Release following Addition of [γ-^{32}P]ATP—Addition of [γ-^{32}P]ATP to recombinant ATP7B is followed by protein phosphorylation, as shown previously (11). Using microsomes obtained from COS1 cells infected with rAdATP7Bmyc, we found that phosphorylation of the ATP7B protein is totally copper-dependent, as no phosphorylation was obtained in the presence of the copper chelator BCS (Fig. 4). Low concentrations of contaminant copper were evidently sufficient to yield maximal phosphorylation, since no additional signal was obtained by addition of $CuCl_2$ up to 10 μM. The phosphorylation levels are somewhat (~20%, as statistically demonstrated in Fig. 5*B*) reduced by running gels with alkaline (pH 8.3) as compared with acid (pH 6.3) buffer (*squares* and *circles* in Fig. 4), indicating that only a fraction of the ATP7B phosphoprotein (obtained by incubation for 15 min with ATP) is alkaline labile. By comparison, the Ca^{2+} ATPase (SERCA1) phosphoenzyme intermediate was completely eliminated by alkaline (pH 8.3) electrophoresis (Fig. 4, *inset*). It is noteworthy that no phosphoenzyme signal was detected by electrophoresis and autoradiography when sham microsomes were incubated with [γ-^{32}P]ATP.

When we measured phosphorylation as a function of time, we found that increasing levels of phosphorylation were obtained within 20–30 min of incubation, with a diphasic pattern, including a faster initial component within the first 2 min (Fig. 5*A*). We then measured the phosphoenzyme formed at a relatively higher rate during the first 2 min, using ATP7B protein subjected to specific mutations. It is shown in Fig. 5*B* that no significant levels of alkali labile phosphoenzyme are formed following the D1027N (putative catalytic phosphorylation site) mutation or C983A/C985A (putative transmembrane copper site at TM6, TMBS) mutations. On the other hand, the C575A/C578A (first putative copper site at the NMBD, *i.e.* closest to the A domain) mutant retained a significant portion of alkali labile phosphoenzyme. It is important to realize that, in Fig. 5*B*, the meaningful difference is that between acid and alkaline electro-

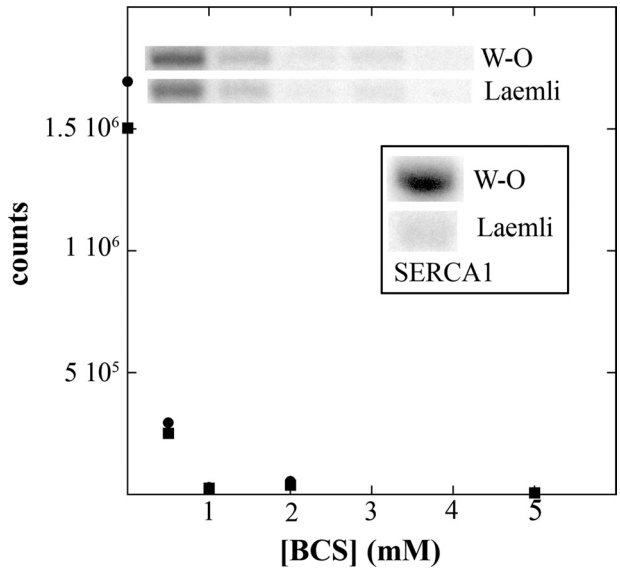

FIGURE 4. **Electrophoretic analysis of ATP7B and SERCA1 phosphorylation by ATP.** Inhibition by BCS and pH stability. ATP7B (50 μg of microsomal protein/ml) was incubated with 50 μM [γ-^{32}P]ATP for 15 min at 37 °C, in a reaction mixture containing 50 mM MES triethanolamine, pH 6.0, 300 mM KCl, 10 mM DTT, 3 mM $MgCl_2$, and either 0, 0.5, 1.0, 2.0, or 5 mM BCS. The samples were quenched with 5% trichloroacetic acid, and the sedimented protein was washed with 0.125 N perchloric acid, and solubilized in 2.5% SDS and 0.5% mercaptoethanol, 3% sucrose, and 0.1 mg of bromphenol blue/ml at pH 6.3 or 8.3. A parallel incubation with SERCA1 (30 μg of light sarcoplasmic reticulum vesicles/ml) was performed for 15 s at 3 °C, in a reaction mixture containing 20 mM MOPS, pH 7.0, 80 mM KCl, 3 mM Mg Cl_2, and 10 μM $CaCl_2$. The solubilized samples (25 μg of protein each) were run on gel electrophoresis with acid (*W–O*) or alkaline (Laemmli) buffer, as described under "Materials and Methods." The figure shows the radioactive bands and the actual radioactivity counts (●, acid electrophoresis; ■, alkaline electrophoresis) obtained by exposure to a Molecular Dynamics storage phosphor screen.

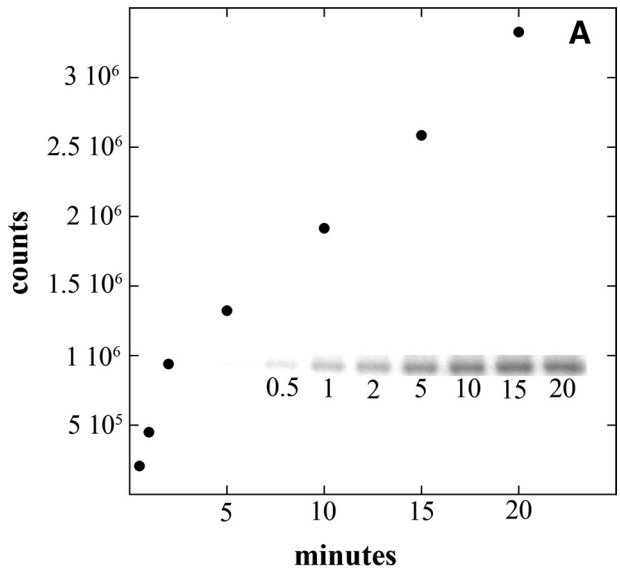

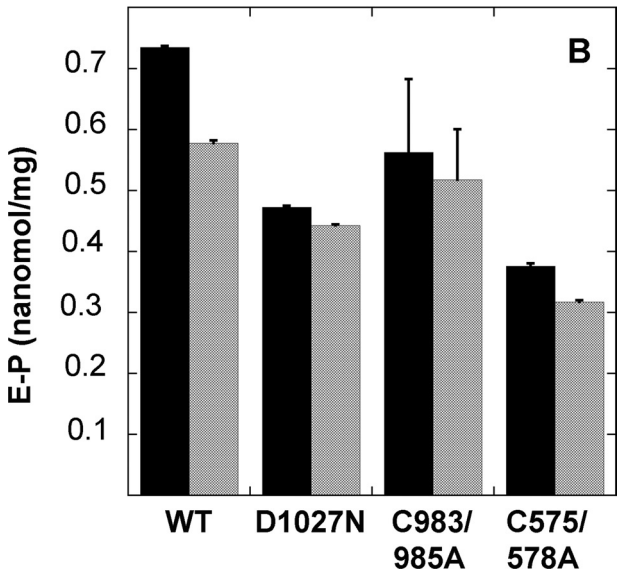

FIGURE 5. **Protein phosphorylation upon addition of 50 μM [γ-^{32}P]ATP to ATP7B WT (*A*) and ATP7B mutants (*B*).** For the time course of phosphorylation, reaction and quenching at various times, solubilization, and electrophoresis were conducted as explained in the legend for Fig. 4. *A*, radioactive bands and the actual radioactivity counts obtained by exposure to a Molecular Dynamics storage phosphor screen. *B*, phosphoenzyme levels obtained following 2-min incubation with 50 μM [γ-^{32}P]ATP, using WT protein, D1027N (putative catalytic phosphorylation site), C983A/C985A (putative transmembrane copper site at TM6), and C575A/c578A (first putative copper site at the NMBD, *i.e.* closest to the A domain) mutants. Results obtained with acid and alkaline electrophoresis are compared.

phoresis for each couple of columns. Differences among various couples are likely to reflect the yield of WT and mutant ATP7B in different microsomal preparations. The absence of alkali labile phosphoenzyme formation in the D1027N and C983A/C985A mutants demonstrates unambiguously that the P-type conserved aspartate and TMBS activating copper are required for catalytic activation.

When we chased with 1 mM non-radioactive ATP the [γ-^{32}P]phosphoenzyme obtained by 2-min incubation with [γ-^{32}P]ATP, we obtained a diphasic decay of the [γ-^{32}P]phosphoenzyme (Fig. 6*A*). The fast component accounts for ~20% of the phosphoenzyme and decays with a half time of 0.2 min (average of several preparations), yielding $k = 3.47\ \text{min}^{-1}$. The alkali-resistant fraction continued to decay at a slower rate. It is of interest that if we added 5 mM BCS in conjunction with the non-radioactive ATP chase, the initial decay was smaller, and then both the alkali labile and alkaline stable fractions remained at the same level, without undergoing further decay (Fig. 6*B*). Furthermore, when we did decay experiments (no BCS added) with the D1027N (putative catalytic phosphorylation site) or C983A/C985A (putative transmembrane copper site at TM6, TMBS) mutant, we observed no early phosphoenzyme decay (Fig. 6, *C* and *D*).

In parallel experiments, at serial times following addition of [γ-^{32}P]ATP, we separated the microsomal protein by filtration, and collected the filters for determination of [^{32}P]phosphoenzyme, and the filtrate for determination of [γ-^{32}P]P_i. As shown in Fig. 7, we found again that [^{32}P]phosphoenzyme is formed with a diphasic pattern. On the other hand, [^{32}P]P_i is released at a linear rate of 4.0 nmol/mg/min protein in these transient state experiments, soon upon formation of the fast (acid stable) phosphoenzyme component, and does not increase any further when additional phosphoenzyme is formed. This rate would be expected considering $k = 3.47\ \text{min}^{-1}$ (see above), and a stoichiometry of ~1.0 nmol of ATPase/mg (as estimated from protein-stained gels and the ATP7B molecular weight). It is noteworthy that in steady-state experiments we obtain a higher velocity (30 nmol/mg/min, see above), likely due to the occur-

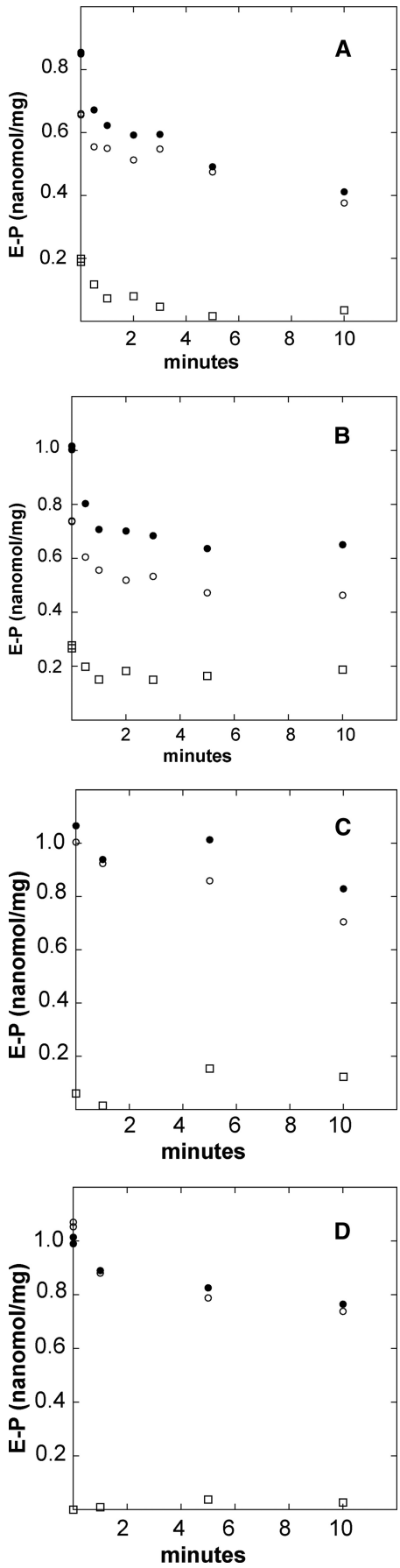

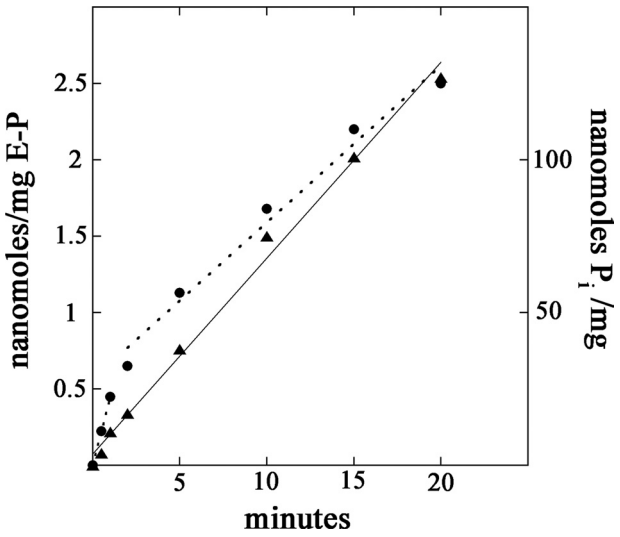

FIGURE 7. **Formation of [γ-^{32}P]phosphoenzyme (●) and hydrolytic cleavage of [γ-^{32}P]P$_i$ (▲) following addition of 50 μM [γ-^{32}P]ATP.** WT ATP7B (50 μg of microsomal protein/ml) was incubated with 50 μM [γ-^{32}P]ATP at 37 °C, in a reaction mixture containing 50 mM MES triethanolamine, pH 6.0, 300 mM KCl, 10 mM DTT, 3 μM $CuCl_2$, and 3 mM $MgCl_2$. Samples were quenched at serial times with 5% trichloroacetic acid and filtered through 0.45-μm Millipore filters under vacuum suction. The filtrate was removed and processed for determination of [^{32}P]P$_i$ (see "Materials and Methods"). The filters were then washed three times with 0.125 N cold perchloric acid, and once with cold water, and used for determination of [γ-^{32}P]phosphoenzyme (see "Materials and Methods").

rence of repeated turnovers and other steady-state factors. In either case, the hydrolytic activity is quite low, as in experiments performed with the Ca^{2+} ATPase (SERCA1) under the same conditions the rates of P$_i$ release are two orders of magnitude higher (22).

Identification of Phosphorylated Residues—The experiments on phosphorylation described above demonstrate stringent copper-dependent phosphorylation, reaching levels higher than 2 nmol/mg of protein following 20–30 min of incubation. This value is higher than expected from the stoichiometry of recombinant ATP7B, which accounts for 10–20% of the microsomal protein and, based on 150-kDa molecular mass, should yield a maximum of 1.0 nmol/mg of protein. We submitted the ATP7B electrophoretic band for mass spectrometric analysis to ascertain information on both the site specific phosphorylation events as well as relative intensities of the phosphorylated sites to the non-phosphorylated form. We expected that phosphorylated serine residues would be more stable than the phosphorylated aspartate within the catalytic domain and might be detected despite the prolonged analytical procedure. In line with our observation of phosphorylation rates far higher than

FIGURE 6. Decay of [γ-^{32}P]phosphoenzyme following a chase with 1 mM non-radioactive ATP in the absence (*A*) or presence (*B*) of 5 mM BCS is shown. WT ATP7B protein was preincubated with 50 μM [γ-^{32}P]ATP for 2 min at 37 °C before addition of 1 mM non-radioactive ATP (*A*), or 1 mM ATP and 5 mM BCS (*B*). In the *lower panels*, D1027N (*C*) or C983A/C985A (*D*) mutants were preincubated with 50 μM [γ-^{32}P]ATP for 2 min at 37 °C before addition of 1 mM non-radioactive ATP. Samples quenched at serial times were then processed for acid or alkaline electrophoresis as explained for Fig. 4. The values given represent the stoichiometry of phosphorylation based on radioactivity standards determined by scintillation counting and are the difference between results obtained with microsomes derived from COS-1 cells infected with rAdATP7Bmyc and from cells infected with rAdGFP (sham).

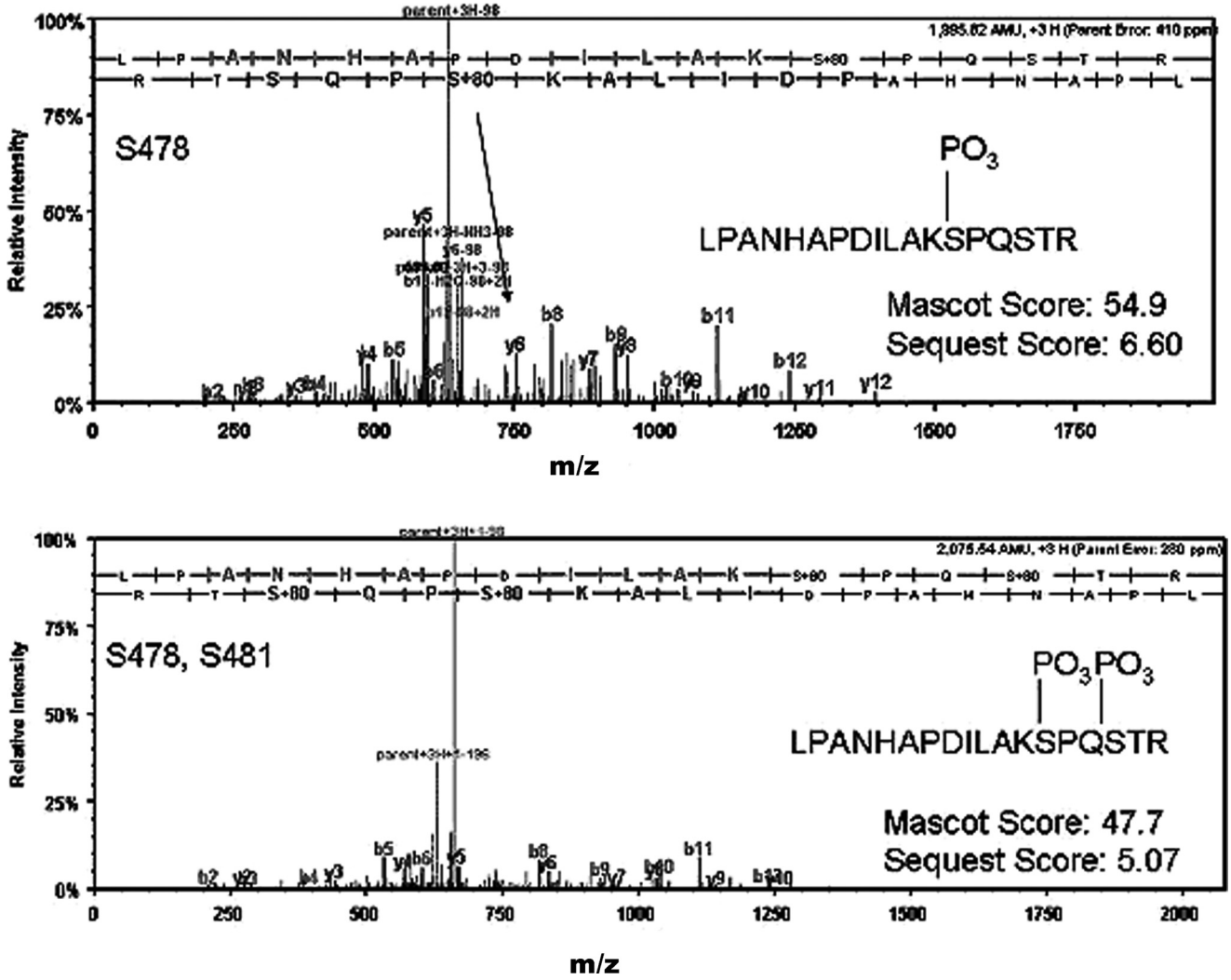

FIGURE 8. **MS/MS fragment ion spectra of a phosphopeptide derived from the NMBD.** The *top panel* shows the mono-phosphorylated form, and the *bottom panel* shows the di-phosphorylated form of the same fragment. The serine phosphorylation sites are pS478 and pS481. Both peptides were identified as triply charged (3^+) cations showing predominant PO_3 loss. The symbol *m/z* reflects mass to charge ratio. The Mascot Score reflects the probability that the observed match is a random event. The SEQUEST score derives from algorithms used to assign peptides by data base searching based on MS/MS spectra acquired by mass spectrometry.

seen without copper induction, is the fact that phosphopeptide identification was done without the need for phosphopeptide enrichment. This experimental protocol is only viable when the phosphorylation events occur at extremely high stoichiometry. In addition, non-enriched phosphopeptide identification allows for relative quantification of both the phosphorylated and non-phosphorylated peptide forms.

MS revealed 44% sequence coverage of the ATP7B molecule, and three unique phosphopeptides with four unique phosphorylation sites. The first phosphopeptide includes mono-phosphorylated Ser^{478} and to a lesser degree doubly phosphorylated Ser^{481} (Fig. 8), it should be noted that the mono-phosphorylated form was only identified as Ser^{478}; in no instances was mono-phosphorylated Ser^{481} identified. Occupancy rate determination (intensity p-form/Sum p-form+Non-p form) could not be determined in this scenario because the miss-cleavage at Lys^{477} (phosphorylated Ser^{478} C-terminal) does not occur in the non-phosphorylated form. The second phosphopeptide revealed phosphorylation of Ser^{1121}, and the occupancy rate was calculated to be 13%. Finally, the third phosphopeptide, Ser^{1453}, was recovered with an occupancy rate of 51%. The phosphorylated serine residues were identified using strict tolerances and in all cases included validation manually (Figs. 8 and 9). The occupancy rates were determined by extraction of the ion intensities of the noted peptides; notably the error in this measurement is inherently large because of the variability in ionization efficiencies.

To unveil whether serine phosphorylation in the expressed ATP7B may be present before isolation of the microsomes, we submitted samples obtained *before* and *after* exposure to [γ-^{32}P]ATP, with the aim of distinguishing phosphorylation that occurred *ex vivo* within the cell, and phosphorylation that occurred upon incubation with ATP *in vitro*. We found that Ser^{478}, Ser^{481}, and Ser^{1453} were phosphorylated in both the *ex vivo* and *in vitro* samples, with a similar occupancy rates. In addition, it is interesting to note that incubation of the ATP7B protein with phosphatase prior to phosphorylation with [γ-^{32}P]ATP results in enhancement in the rate and level of

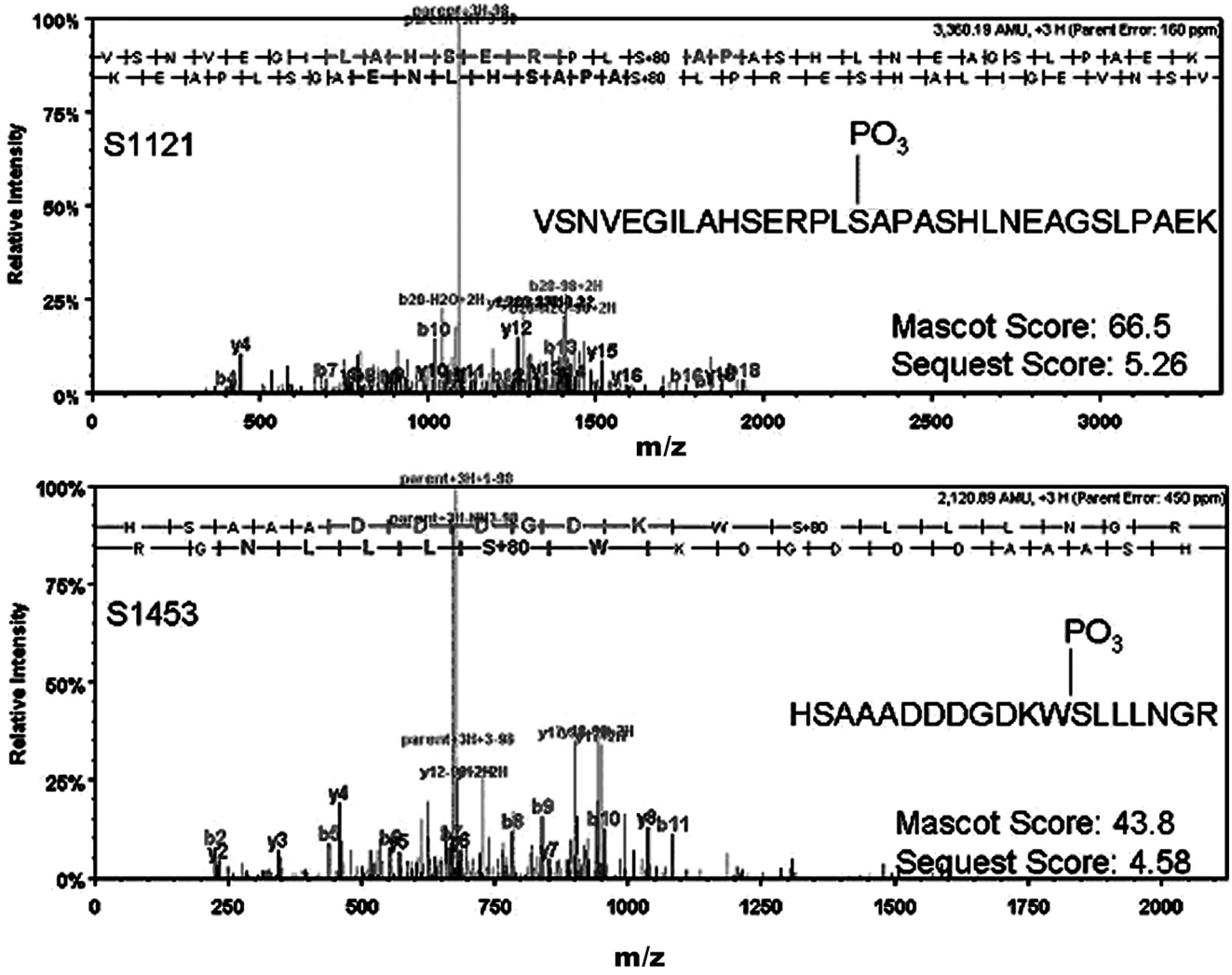

FIGURE 9. **MS/MS fragment ion spectra of two phosphopeptides derived from the N domain and the C terminus, respectively.** The serine phosphorylation sites are pS1121 (*top panel*) and pS1453 (*bottom panel*). In the phosphopeptide VSNVEGILAHSERPLSAPApSHLNEAGSLPAEK, the expected cleavage at Arg^{1114} does not occur as Arg^{1114} resides N-terminal to proline. Both phosphopeptides were identified as triply charged (3^+) cations. *Symbols* are as in the legend for Fig. 8.

phosphorylation *in vitro* (Fig 10). These findings further support the existence of *ex vivo* phosphorylation, whereby hydrolytic cleavage may be rate-limiting for their phosphorylation of the same residues *in vitro*.

DISCUSSION

The ATP7B protein presents sequence homologies that are conserved through all P-ATPases, including residues within the nucleotide binding ("N") domain and the phosphorylation ("P") domain. Therefore, it is tempting to assume that the catalytic and transport mechanism is analogous to that of well characterized cation transport ATPases, such as the Ca^{2+} ATPase (SERCA) and the Na^+/K^+ ATPase (8, 23, 24). In fact, copper-dependent phosphorylation of recombinant ATP7B protein by utilization of ATP has been reported (11) and attributed in part to formation of phosphorylated enzyme intermediate and in part to additional phosphorylation of serine residues. Here we confirm occurrence of phosphorylation, and, taking advantage of the high yield expression, we demonstrate the copper dependence (Fig. 4) and define the time course of phosphoenzyme formation as well as its decay following a chase with non-radioactive ATP (Figs. 6 and 7). The kinetics of phosphoenzyme formation is diphasic, with an alkali-labile fraction formed within the first 2 min of reaction. The alkali-labile phosphoenzyme is not obtained with the D1027N (putative catalytic phosphorylation site) mutant or C983A/C985A (putative transmembrane copper site at TM6) mutant. This demonstrates its identity as a phosphorylated intermediate analogous to that found in other P-type ATPases, which involves phosphorylation of an aspartyl residue within a conserved sequence of the P domain, and requires activation by copper bound to the transmembrane site. In addition, the phosphoenzyme undergoes diphasic decay, and the alkali-labile fraction decays in the early phase (Fig. 6*A*). This early decays is not observed when the D1027N or C983A/C985A mutant is used (Fig. 6, *C* and *D*). Finally, we find that the P_i release obtained following addition of [γ-^{32}P]ATP to ATP7B begins in concomitance with the fast phase of phosphoenzyme formation and continues at a linear rate thereafter (Fig. 7). This indicates that the phosphoenzyme formed within the fast phase is the catalytic intermediate. In fact, if the high level of [^{32}P]phosphoenzyme formed in the

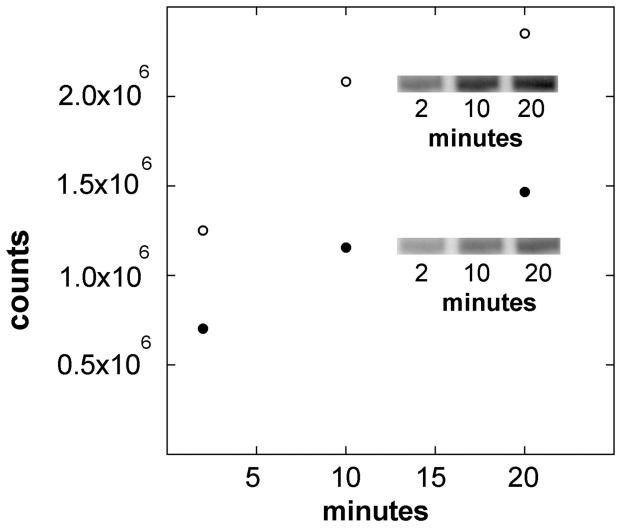

FIGURE 10. **Reduction of *ex vivo* phosphorylated levels by λ-protein phosphatase *in vitro*, and [γ-^{32}P]phosphoenzyme formation *in vitro*.** WT ATP7B was incubated for 30 min at 30 °C, in the presence (○) or the absence (●) of λ-protein phosphatase (see "Materials and Methods"). Following centrifugation and resuspension in medium 3, ATP7B (50 μg of microsomal protein/ml) was incubated with 50 μM [γ-^{32}P]ATP at 37 °C, in a reaction mixture containing 50 mM MES triethanolamine, pH 6.0, 300 mM KCl, 10 mM DTT, 3 μM $CuCl_2$, and 3 mM $MgCl_2$. Samples were quenched at serial times with 5% trichloroacetic acid, and the solubilized protein was subjected to Weber-Osborn electrophoretic analysis. The radioactive bands and the radioactivity counts obtained by exposure to a Molecular Dynamics storage phosphor screen are shown in the figure.

slower phase were a catalytic intermediate, P_i release would occur with a lag period, acquiring high rate only after maximal levels of phosphoenzyme are reached. It is noteworthy that the phosphorylated ATP7B protein is only partially degraded by alkaline pH, whereas the Ca^{2+} ATPase phosphoenzyme is totally degraded (Fig. 4). Finally, consider that the phosphorylation levels exceed the stoichiometry of the ATP7B protein present in the microsomal preparation (see "Results"), indicating phosphorylation in excess of one residue per ATP7B molecule and heterogeneity of the phosphorylation sites.

Both transient and steady-state measurements indicate a very low rate of hydrolytic cleavage, which is approximately two orders of magnitude lower than that obtained in comparable experiments performed with the Ca^{2+} ATPase (SERCA1) under the same conditions (22). However, it should be pointed out that hydrolytic cleavage of the SERCA phosphoenzyme is strongly reduced when the Ca^{2+} concentration is raised above the millimolar concentration. This phenomenon, referred to as "back inhibition," is due to interference with net dissociation of bound Ca^{2+} from the transport sites, whereby the phosphoenzyme is restricted from shifting to the calcium free state, which is the state undergoing hydrolytic cleavage. In the case of ATP7B, we consider unlikely that strongly bound copper is easily released as free Cu^{+} from the phosphoenzyme into the medium creating a concentration gradient (25), but may be rather released to a specific acceptor for copper dissociation from the TMBS under physiological conditions (26). Therefore,

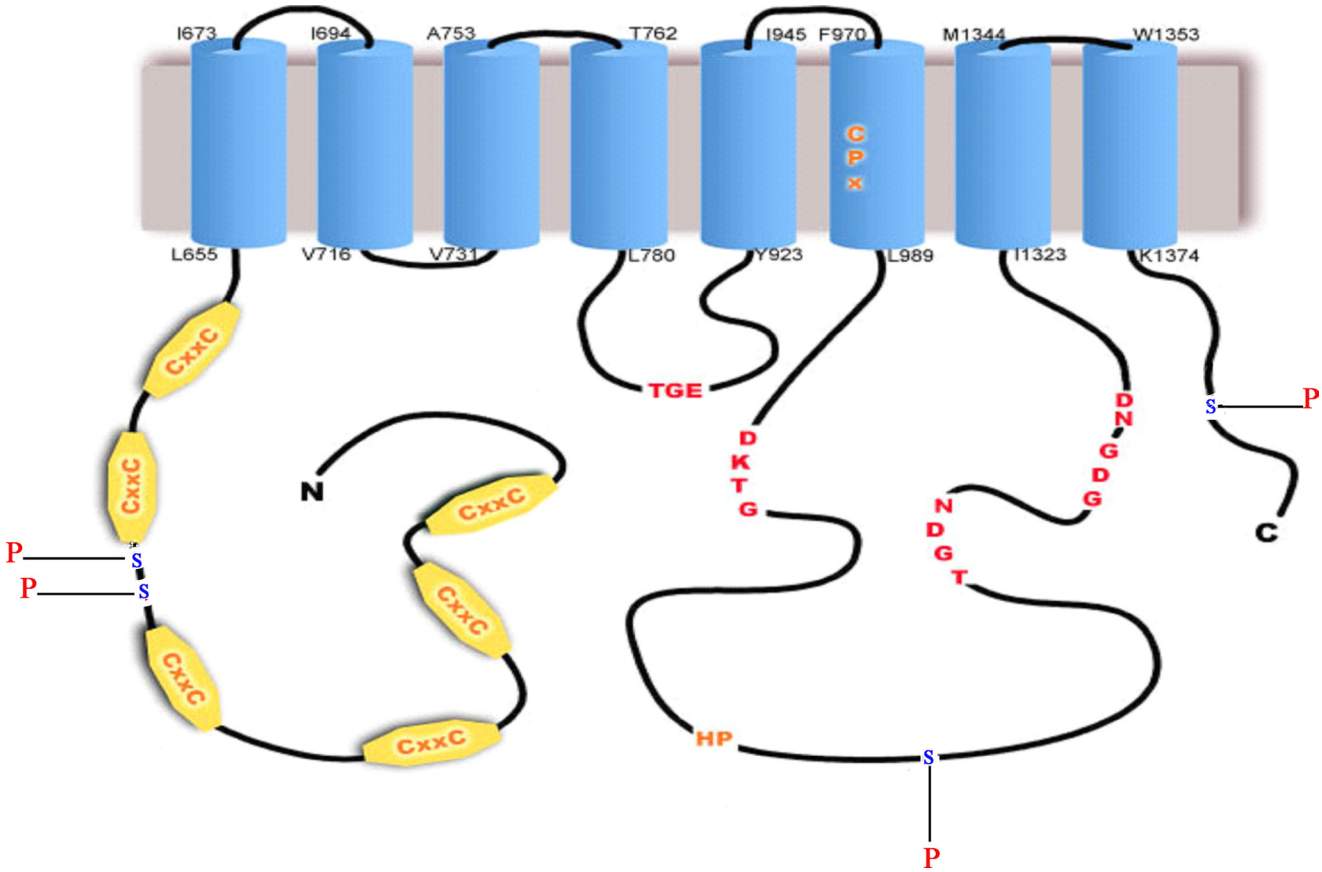

FIGURE 11. **Two-dimensional folding model of the ATP7B sequence, showing serine residues undergoing phosphorylation.** The position of phosphorylated serine residues, demonstrated by phosphopeptide analysis using MS, is shown in the ATP7B sequence modeled as proposed by Lutsenko *et al.* (1).

cleavage of ATP7B phosphoenzyme in our conditions may be "back-inhibited" by the prolonged *on time* of copper bound to the TMBS. On the other hand, when we add a copper chelator (Fig. 6*B*), phosphoenzyme decay is totally inhibited, because copper is dissociated not only from the TMBS but also from the NMBD. In fact, it was shown that in bacterial CopA dissociation of copper allows interaction of empty NMBD with the A domain, with consequent inhibition of phosphoenzyme decay (30). A most important conclusion is that activation of ATP7B depends on copper binding to the TMBS as well as to the NMBD.

Another aspect of our experiments is related to identification of residues undergoing phosphorylation at rates lower than the phosphoenzyme intermediate, and reaching levels higher than the enzyme stoichiometry in the microsomal preparation. In fact, evidence for a phosphorylation site between Met^{796} and Ser^{1384} of ATP7B within liver cells *in situ* was previously reported (10), and the possible phosphorylation of several residues in recombinant ATP7B was indicated (27, 28). Taking advantage of the high yield expression of ATP7B in COS-1 cells infected with rAdATP7Bmyc, we proceeded to identify by phosphoproteomic analysis and mass spectrometry the specific residues undergoing copper-dependent phosphorylation upon addition of ATP to our microsomal preparations. We found that Ser^{478} and Ser^{481} were phosphorylated within the NMBD, Ser^{1121} within the N domain, and Ser^{1453} within the C terminus (Fig. 11). Reliable phosphorylation signal on Asp^{1027}, the putative residue undergoing phosphorylation as an intermediate in the catalytic cycle, was not detected. This is possibly due to hydrolytic cleavage during the long procedure of proteolysis, peptide separation, and mass spectrometry. It is noteworthy that a fairly high phosphorylation level of the serine residues was already found even before incubation of the microsomes with ATP *in vitro*, indicating occurrence of phosphorylation within the cultured cells *in situ*. Therefore, the slow phosphorylation of serine residues with [γ-^{32}P]ATP *in vitro* reflects a requirement for dephosphorylation before exchange with [^{32}P]PO_4 can take place. In fact, incubation of microsomes with phosphatase previous to exposure to [γ-^{32}P]ATP increases early formation of [^{32}P]phosphoenzyme (Fig. 10).

It has been proposed that phosphorylation of serine residues plays an important role in copper homeostasis, promoting functional interactions of cuproenzymes (2). It is noteworthy that phosphorylation of ATP7B in human cells is copper-dependent (10), and this phosphorylation appears to play an important role in copper homeostasis and ATP7B trafficking within the cell. In agreement with these findings, we find that phosphorylation of recombinant ATP7B in our microsomal preparation is totally copper-dependent. It is possible that ATP7B phosphorylation sites become exposed as a consequence of copper-induced conformational changes (2). It is also apparent that serine phosphorylation plays a role in regulation of the copper ATPase catalytic cycle. In fact, it was reported that the activity of yeast copper ATPase Ccc2p is regulated by Ser^{258} phosphorylation (29). Our finding of two phosphorylated serines (Ser^{478} and Ser^{481}) within the NMBD is intriguing, because the NMBD of ATP7B undergoes copper-dependent conformational changes and interaction with chaperone proteins (31).

REFERENCES

1. Lutsenko, S., Barnes, N. L., Bartee, M. Y., and Dmitriev, O. Y. (2007) *Physiol. Rev.* **87,** 1011–1046
2. Veldhuis, N. A., Gaeth, A. P., Pearson, R. B., Gabriel, K., and Camakaris, J. (2009) *Biometals* **22,** 177–190
3. Vulpe, C., Levinson, B., Whitney, S., Packman, S., and Gitschier, J. (1993) *Nat. Genet.* **3,** 7–13
4. Tanzi, R. E., Petrukhin, K., Chernov, I., Pellequer, J. L., Wasco, W., Ross, B., Romano, D. M., Parano, E., Pavone, L., Brzustowicz, L. M., Devoto, M., Peppercorn, J., Bush, A. I., Sternlieb, I., Pirastu, M., Gusella, J. F., Egrafov, O., Penchszadeh, G. K., Honig, B., Edelman, I. S., Soares, M. B., Scheinberg, I. M., and Gilliam, T. C. (1993) *Nat. Genet.* **4,** 344–350
5. Bull, P. C., Thomas, G. R., Rommens, J. M., Forbes, J. R., and Cox, D. W. (1993) *Nat. Genet.* **4,** 327–337
6. Yamaguchi, Y., Heiny, M. E., and Gitlin, J. D. (1993) *Biochem. Biophys. Res. Commun.* **197,** 271–277
7. Burroughs, A. M., Allen, K. N., Dunaway-Mariano, D., and Aravind, L. (2006) *J. Mol. Biol.* **361,** 1003–1034
8. Lutsenko, S., and Kaplan, J. H. (1995) *Biochemistry* **34,** 15607–15613
9. Palmgren, M. G., and Axelsen, K. B. (1998) *Biochim. Biophys. Acta* **1365,** 37–45
10. Vanderwerf, S. M., Cooper, M. J., Stetsenko, I. V., and Lutsenko, S. (2001) *J. Biol. Chem.* **276,** 36289–36294
11. Tsivkovskii, R., Eisses, J. F., Kaplan, J. H., and Lutsenko, S. (2002) *J. Biol. Chem.* **277,** 976–983
12. Hung, Y. H., Layton, M. J., Voskoboinik, I., Mercer, J. F., and Camakaris, J. (2007) *Biochem. J.* **401,** 569–579
13. He, T. C., Zhou, S., da Costa, L. T., Yu, J., Kinzler, K. W., and Vogelstein, B. (1998) *Proc. Natl. Acad. Sci. U.S.A.* **95,** 2509–2514
14. Smart, S. C., Sagar, K. B., el, Schultz, J., Warltier, D. C., and Jones, L. R. (1997) *Cardiovasc. Res.* **36,** 174–184
15. Laemmli, U. K. (1970) *Nature* **227,** 680–685
16. Weber, K., and Osborn, M. (1969) *J. Biol. Chem.* **244,** 4406–4412
17. Eletr, S., and Inesi, G. (1972) *Biochim. Biophys. Acta* **282,** 174–179
18. Lanzetta, P. A., Alvarez, L. J., Reinach, P. S., and Candia, O. A. (1979) *Anal. Biochem.* **100,** 95–97
19. Mazanek, M., Mituloviae, G., Herzog, F., Stingl, C., Hutchins, J. R., Peters, J. M., and Mechtler, K. (2007) *Nat. Protoc.* **2,** 1059–1069
20. Braiterman, L., Nyasae, L., Guo, Y., Bustos, R., Lutsenko, S., and Hubbard, A. (2009) *Am. J. Gastroenterol.* **296,** 433–444
21. Takeda, K., Ushimaru, M., Fukushima, Y., and Kawamura, M. (1999) *J. Membr. Biol.* **170,** 13–16
22. Fernandez-Belda, F., Kurzmack, M., and Inesi, G. (1984) *J. Biol. Chem.* **259,** 9687–9698
23. de Meis, L., and Vianna, A. L. (1979) *Annu. Rev. Biochem.* **48,** 275–292
24. Toyoshima, C., and Inesi, G. (2004) *Annu. Rev. Biochem.* **73,** 269–292
25. Kim, B. E., Nevitt, T., and Thiele, D. J. (2008) *Nat. Chem. Biol.* **4,** 176–185
26. Lutsenko, S., Gupta, A., Burkhead, J. L., and Zuzel, V. (2008) *Arch. Biochem. Biophys.* **476,** 22–32
27. Vanderwerf, S. M., and Lutsenko, S. (2002) *Biochem. Soc. Trans.* **30,** 739–741
28. Bartee, M. Y., Ralle, M., Lutsenko, S. (2009) *Biochemistry* **48,** 5573–5581
29. Valverde, R. H., Morin, I., Lowe, J., Mintz, E., Cuillel, M., and Vieyra, A. (2008) *FEBS Lett.* **582,** 891–895
30. Hatori, Y., Hirata, A., Toyoshima, C., Lewis, D., Pilankatta, R., and Inesi, G. (2008) *J. Biol. Chem.* **283,** 22541–22549
31. Banci, L., Bertini, I., Cantini, F., Rosenzweig, A. C., and Yatsunyk, L. A. (2008) *Biochemistry* **47,** 7423–7429